AGU ADVANCING EARTH AND SPACE SCIENCES

Geophysical Research Letters

RESEARCH LETTER
10.1029/2024GL111490

Synoptic Scale Controls and Aerosol Effects on Fog and Low Stratus Life Cycle Processes in the Po Valley, Italy

Eva Pauli[1,2], Jan Cermak[1,2], Jörg Bendix[3], and Philip Stier[4]

[1]Institute of Meteorology and Climate Research, Karlsruhe Institute of Technology (KIT), Karlsruhe, Germany, [2]Institute of Photogrammetry and Remote Sensing, Karlsruhe Institute of Technology (KIT), Karlsruhe, Germany, [3]Faculty of Geography, Laboratory for Climatology and Remote Sensing, University of Marburg, Marburg, Germany, [4]Atmospheric, Oceanic and Planetary Physics, Department of Physics, University of Oxford, Oxford, UK

Abstract Fog and low stratus clouds (FLS) form as a result of complex interactions of multiple factors in the atmosphere and at the land surface and impact both the anthropogenic and natural environments. Here, we analyze the role of synoptic conditions and aerosol loading on FLS occurrence and persistence in the Po valley in northern Italy. By applying k-means clustering to reanalysis data, we find that FLS formation in the Po valley is either based on radiative processes or moisture advection from the Mediterranean sea. Satellite-based data on FLS persistence shows longer persistence of radiatively formed FLS events, likely due to air mass stagnation and a temperature inversion. Ground-based aerosol optical depth observations further reveal that FLS event duration is significantly higher under high aerosol loading. The results underline the combined effect of topography, moisture advection and aerosol loading on the FLS life cycle in the Po valley.

Plain Language Summary Fog and low stratus clouds (FLS) are influenced by various drivers in the atmosphere and near the ground. Here, the impact of the large-scale weather situation and aerosols is analyzed over the Po valley in northern Italy. Using reanalysis and satellite data we find that FLS events driven by nighttime cooling under stable conditions can persist longer than FLS events formed as a result of moisture transport. Investigating ground-based observations of aerosols, particles on which moisture can condensate and fog and cloud droplets form, we find that FLS event duration is higher when a higher amount of aerosols is present. These results can help when predicting the duration of FLS events, which is particularly important for traffic safety.

Key Points:

- Fog and low stratus (FLS) cloud formation in the Po valley is primarily controlled by radiative processes or moisture advection
- FLS persistence from the satellite perspective is highest for radiatively formed FLS events likely due to a stable boundary layer
- FLS persistence is significantly higher under high aerosol loading

Supporting Information:

Supporting Information may be found in the online version of this article.

Correspondence to:

E. Pauli,
eva.pauli@kit.edu

Citation:

Pauli, E., Cermak, J., Bendix, J., & Stier, P. (2024). Synoptic scale controls and aerosol effects on fog and low stratus life cycle processes in the Po valley, Italy. *Geophysical Research Letters*, *51*, e2024GL111490. https://doi.org/10.1029/2024GL111490

Received 19 JUL 2024
Accepted 7 OCT 2024

Author Contributions:

Conceptualization: Eva Pauli, Jan Cermak, Philip Stier
Formal analysis: Eva Pauli
Investigation: Eva Pauli
Methodology: Eva Pauli, Jan Cermak
Visualization: Eva Pauli
Writing – original draft: Eva Pauli
Writing – review & editing: Eva Pauli, Jan Cermak, Jörg Bendix, Philip Stier

1. Introduction

Fog, defined as a suspension of water droplets reducing visibilities to less than 1,000 m at or near the ground (American Meteorological Society, 2012; Glickman, 2000), impacts the natural and anthropogenic environments in multiple ways. While the reduction in visibility poses a threat to traffic safety (Dietz et al., 2019; Kneringer et al., 2019; Leigh et al., 1998; Pagowski et al., 2004) and reduces solar power input (Köhler et al., 2017), fog also preserves biodiversity by serving as a water input in otherwise arid ecosystems (Gottlieb et al., 2019; Mitchell et al., 2020) and fog regions can even serve as climate change refugia (Pohl et al., 2023).

Fog occurrence and life cycle (formation and dissipation) are primarily influenced by the synoptic situation (Bendix, 1994; Egli et al., 2019; Gultepe et al., 2007), that is, the pressure field (Pauli et al., 2020; Ye, 2009) and near ground conditions such as temperature, wind speed and the height of the boundary layer (Cuxart & Jiménez, 2012; Pauli et al., 2020; Pérez-Díaz et al., 2017; Price, 2019). While radiation fog typically forms in calm, high-pressure conditions (Bergot, 2016; Roach, 1995), steady winds are required for the formation of advection fog (Gultepe et al., 2007). Land surface conditions, for example, topography and land cover further modify the fog life cycle (Fuchs et al., 2022; Gautam & Singh, 2018; Pauli, Cermak, & Teuling, 2022; Scherrer & Appenzeller, 2014). A major component of fog formation at the interface of atmosphere and land surface are aerosols. Aerosols provide cloud condensation nuclei (CCN) at which water vapor condenses and fog droplets form (Poku et al., 2019; Ramanathan et al., 2001). Particularly aerosol-cloud interactions (ACI), specifically an increase in CCN due to an increase in aerosol amount (Twomey, 1977) has been found to increase fog lifetime and delay fog dissipation (Maalick et al., 2016; Mass et al., 2024; Stolaki et al., 2015; Yan et al., 2020, 2021). While aerosol-radiation interactions (ARI) can lead to earlier fog dissipation through a temperature increase due to aerosol absorption (Anurose et al., 2024), the reflection of radiation in polluted conditions can also increase the boundary layer stability, thereby promoting fog formation (Gao et al., 2015).

Both frequent fog occurrence and high aerosol loadings can be observed in the Po valley, located in northern Italy. The Po valley is one of the most polluted areas in Europe (Di Antonio et al., 2023) due to high emissions from traffic, biomass burning and agriculture (Scotto et al., 2021) in combination with mountain ranges to the north, east and south leading to air mass stagnation and accumulation of pollutants (Putaud et al., 2014). This unique location in combination with continental air masses leads to radiation fog formation as well as to fog formation as a result of the advection of moist air masses from the Mediterranean particularly in winter (Bendix, 1994; Wobrock et al., 1992). While a number of studies have investigated the fog water chemistry in the Po valley, detecting high pollution levels (e.g., Fuzzi et al., 1996; Gilardoni et al., 2014; Giulianelli et al., 2014), no analysis on the effect of aerosol loading on the fog life cycle in the Po valley exists to date.

The aim of this study is to investigate the impact of both synoptic conditions and aerosol loading on fog formation and duration in the Po valley, a combination which has not been studied over large spatial and temporal scales previously. To obtain a complete spatial perspective on fog over the study area, satellite-based data sets of fog occurrence and life cycle are used (Egli et al., 2017; Pauli, Cermak, & Andersen, 2022; Pauli et al., 2021). From the satellite perspective, fog is treated as one category with low stratus clouds (fog and low stratus: FLS) as a separation of the two is irrelevant for a number of application and technically challenging (Cermak et al., 2009). In the context of this study, FLS is therein defined as a low stratiform cloud with liquid droplets which do not exceed a size of 20 μm (Egli et al., 2017). Using these satellite-based FLS data sets in combination with reanalysis data and ground-based aerosol measurements we analyze FLS occurrence and life cycle in winter (DJF) from 2006 to 2015. Through k-means clustering, we aim to answer (a) which types of FLS formation mechanisms exist in the Po valley in terms of the large-scale meteorological conditions and (b) if aerosol loading has an influence on FLS persistence in the identified FLS types.

2. Data and Methods

2.1. Data

In this study, satellite-based data sets on FLS occurrence and life cycle from 2006 to 2015 (Egli et al., 2017; Pauli, Cermak, & Andersen, 2022; Pauli et al., 2021, 2024), reanalysis data from ERA5 (Hersbach et al., 2023a, 2023b) and ground-based aerosol observations (Holben et al., 1998) are used (cf. Figure S1 in Supporting Information S1).

The data set on FLS occurrence (Egli et al., 2017) is based on the Satellite-based Operational Fog Observation Scheme (SOFOS) by Cermak and Bendix (2007); Cermak and Bendix (2008), which primarily uses the reflective properties of FLS in the 3.9 μm, 8.7 μm, 10.8 μm and 12.0 μm channels, to separate FLS from clear sky and other clouds by testing for cloud presence, phase, stratiformity and height. The scheme is then applied to Meteosat SEVIRI with a spatial resolution of 3×3 km at nadir and a temporal resolution of 15 min. Data on FLS formation time, dissipation time and duration is taken from the data set developed in Pauli, Cermak, and Andersen (2022), which is created by applying logistic regression to FLS time series from the aforementioned FLS data set by Egli et al. (2017). The spatial extent of FLS life cycle regimes is taken from the results from Pauli et al. (2024), which have been created by clustering sensitivities of FLS formation and dissipation time from Pauli, Cermak, and Andersen (2022) to environmental conditions.

To identify and explain different FLS formation mechanisms over the Po valley, ERA5 reanalysis data with a spatial resolution of $0.25° \times 0.25°$and a temporal resolution of 1 hr is used. Parameters used are temperature (T), relative humidity (RH) and winds (u, *v*, w) on pressure levels (Hersbach et al., 2023a) and mean surface pressure (msp) and *u* and *v* at 10 m height (Hersbach et al., 2023b). For information on the abundance of aerosols, total aerosol optical depth (AOD) and the angstrom exponent (AE) at 500 nm from AERONET (Aerosol robotic network) at the stations in Modena, Venice and Ispra are used (Holben et al., 1998). These data are based on the spectral deconvolution algorithm (O'Neill et al., 2003), are quality controlled and available at daylight. Though AERONET data is only available at clear sky, the measurement rate is high (>1 measurements per hour), providing measurements also in short cloud-free periods, resulting in a higher temporal coverage than frequently used satellite-based aerosol retrievals (e.g., Lyapustin et al., 2018).

2.2. Methods

In a first step, data on FLS occurrence from Egli et al. (2017) are used to select FLS events regionally constrained to the Po valley and exclude large-scale low stratus situations. This is done by selecting only those winter (DJF)

days where FLS in the Po valley regime lasts twice as long as in two alpine FLS regimes based on Pauli et al. (2024). This results in 430 days available for analysis.

These events are difficult to distinguish further solely from the satellite perspective. Therefore, the latitudinal RH profiles from ERA5 on those 430 days, on the pressure levels 550–1,000 hPa, from 44°N to 46°N and averaged over 11.25°E–12.25°E, are then used to group FLS events with similar FLS formation mechanisms. The profiles are extracted at 6 a.m. UTC as most FLS events are developing at that time and reach their maximum extent shortly after sunrise (Bendix, 1994). Solely these RH profiles are then used as an input into k-means clustering (Hartigan & Wong, 1979) as FLS events with similar relative humidity profiles are likely based on similar FLS formation pathways. We then apply silhouette analysis (Rousseeuw, 1987) to choose a suitable number of clusters, revealing two clusters as the best choice (Figure S2 in Supporting Information S1).

For the two identified clusters, the average duration of FLS events, as well as the spatial patterns of FLS formation and dissipation from Pauli, Cermak, and Andersen (2022) are then analyzed. The latter are displayed as the average temporal rank of FLS formation and dissipation described in detail in the Supporting Information. In addition T and RH profiles and msp and winds from ERA5 are used to explain synoptic scale controls of FLS formation processes.

Lastly, the effect of aerosol loading (approximated by the aerosol index) on the FLS life cycle, is analyzed for FLS events at AERONET stations in Modena, Venice and Ispra. The aerosol index (AI), that is, AOD multiplied by AE, provides a size independent estimate of aerosol loading and potential CCN (Gryspeerdt et al., 2014; Nakajima et al., 2001). FLS event duration from the FLS life cycle data set (Pauli, Cermak, & Andersen, 2022; Pauli et al., 2021) is then averaged over a 3×3 pixel area, centered over the AERONET station. Although other studies have investigated aerosol effects on formation and/or dissipation time (cf. Mass et al., 2024; Yan et al., 2021), we use FLS duration here, as FLS formation and dissipation have a high variability (cf. Figure S3 in Supporting Information S1), making it challenging to attribute shifts in formation and dissipation time to changes in AI.

To analyze if AI has an effect on the FLS life cycle, FLS duration is analyzed on high and low AI days based on the 75th and 25th percentile of the 1 day rolling mean prior to FLS formation. To include the temporal development of AI before FLS forms, rolling means of AI from 1 up to 10 days prior to FLS formation are analyzed for high and low duration events (75th and 25th percentile of FLS duration). Rolling 1 to 10 day means of AI before FLS forms are used here to increase the availability of data points and reduce the short term variability in the AI data. As a quality control measure, valid 1 day rolling means of AI have to be present at least 48 hr before FLS formation occurs, leading to 209 out of 460 FLS events at these locations. 20 outliers ($>\pm 1.5 * IQR$ (interquartile range)) are excluded, leading to 189 FLS events for this analysis.

3. Results and Discussion

3.1. FLS Occurrence and Life Cycle Analysis

The average FLS duration, formation and dissipation over all selected days is shown in Figures 1a–1c. FLS events are on average about 10 hr long and can last up to 20 hr in the central-western part of the study area close to the Po river. FLS duration decreases with increasing distance to the river and elevation (Figure 1a). This pattern is in line with satellite-derived fog frequencies shown in Bendix (1994) and visibility observations in Fantuzi (1987), showing increased fog frequencies in the central part of the Po valley. FLS duration is low over the urban area of Milan (45.5°N, 9.2°E) which is likely due to the urban heat island effect, leading to later formation and earlier dissipation, particularly in long (>20 hr) FLS events (Fuchs et al., 2022; Gautam & Singh, 2018; Yan et al., 2020).

Close to the Po river, especially between 9°E and 10°E earlier formation and later dissipation results in high FLS duration, which is likely due to an increased moisture availability (Fuzzi et al., 1996). Earlier FLS formation and therefore higher persistence can be attributed to mesoscale effects, particularly cold air pool formation through katabatic flows from the Alps and the Appenines as proposed in Bendix (1993). Higher FLS persistence at 9°E–10°E is likely due to higher vertical extent of FLS layers in this region due to the smaller extent of the Po valley here (Bendix, 1994). In contrast, FLS persistence in the Alps and Appennines is lower, as FLS dissipates earlier due to a lower vertical extent, faster burn-off and entrainment of warm air from the mountain slopes into the FLS layers.

Figures 1d–1i show the average FLS duration and formation and dissipation times for the FLS events of the two identified clusters. FLS events in cluster 1 last on average for more than 10–20 hr in large areas of the Po valley

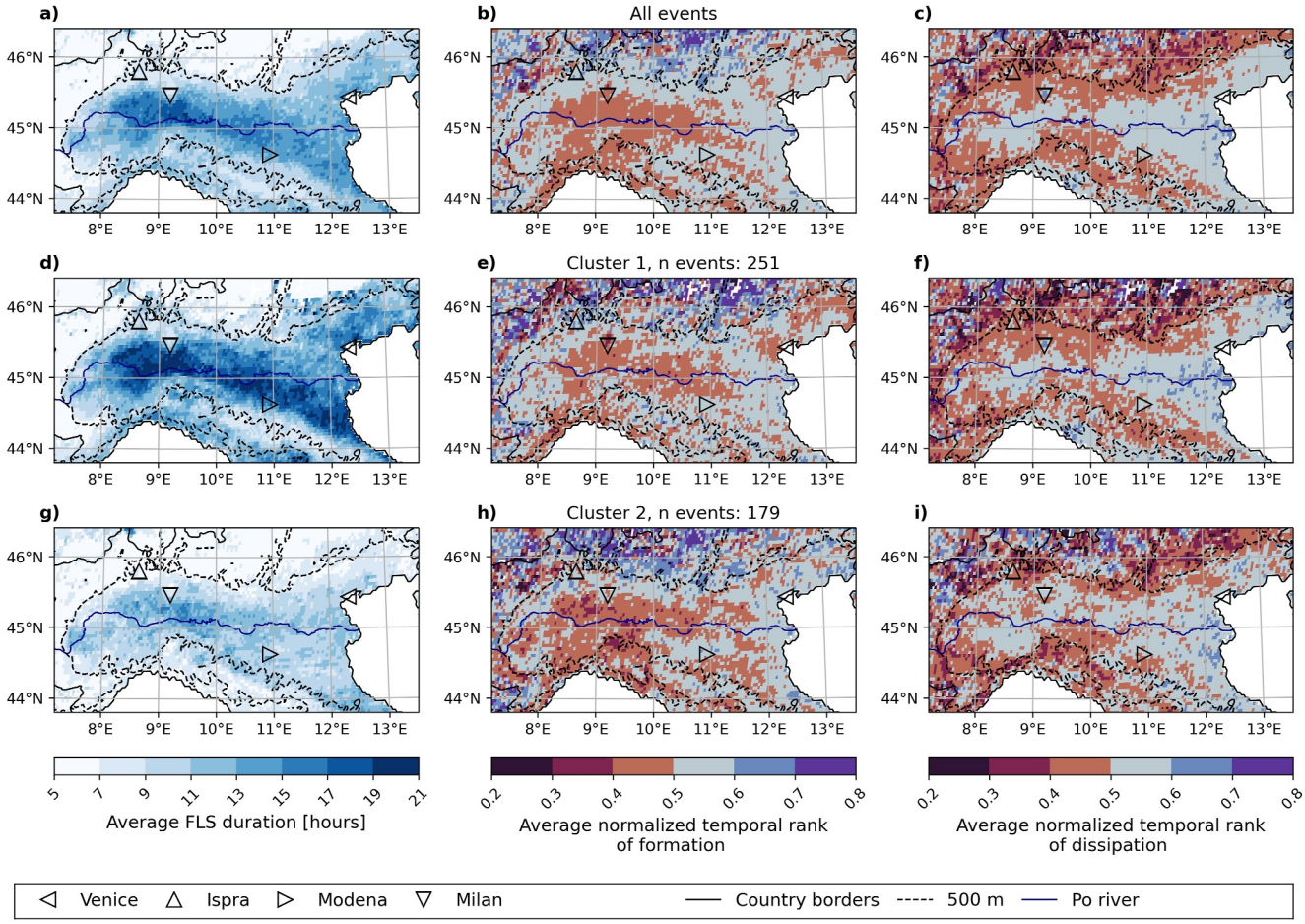

Figure 1. Average FLS event duration (a, d, g), the average temporal rank of formation (b, e, h) and dissipation (c, f, i) for all 430 FLS events (upper row), for cluster 1 (middle row) and cluster 2 (lower row). Country borders are black, the 500 m height contour shown as a dashed line, the Po river as a dark blue line. AERONET stations and Milan are marked as triangles.

and form earlier and dissipate later in the central part of the Po valley close to the river. FLS forms later at the Adriatic coast which is likely due to high sea surface temperatures, absence of the cross valley katabatic flows, and the later onset of along valley cold air drainage flows (Bendix, 1993). FLS events assigned to cluster 2 are shorter (≈7–9 hr on average), with small differences in formation and dissipation time patterns.

3.2. Synoptic Scale Controls of FLS Formation

The cluster specific averages of msp and near-surface winds (u,v) (Figure 2) as well as the vertical profiles of RH and T (Figure 3) help in explaining the observed differences in the FLS life cycle between cluster 1 and 2. FLS events assigned to cluster 1 are likely of radiative origin. High pressure dominates over central Europe (Figures 2a and 2b) leading to a build up of a temperature inversion (Figure 3a, T_{975hPa}-$T_{1000hPa}$≈0.6 K at 45°N) and increased RH near the ground (Figure 3b). The temperature inversion is stronger in the western Po valley, leading to a higher inversion height and consequently a higher vertical fog extent resulting in longer FLS event duration (compare Figure 1) (Bendix, 1993). Stable and high pressure conditions are well known to be beneficial for radiation fog formation (Egli et al., 2019; Pauli et al., 2020; Ye, 2009) and have been identified for the Po valley explicitly by Bendix (1994) and Wobrock et al. (1992), though lacking the extensive spatial vertical view provided here. The upper boundary layer and the free troposphere are on average 10%–15% drier and 1 K warmer than the overall mean (Figures 3c and 3d). In the boundary layer, wind speeds are low but increase in the free troposphere where air masses descend on the alpine slopes. The positive influence of a dry free troposphere on FLS occurrence has also been identified over the Namib region, as it increases longwave radiative cooling of the boundary layer, leading to high persistence of FLS layers (Andersen et al., 2020).

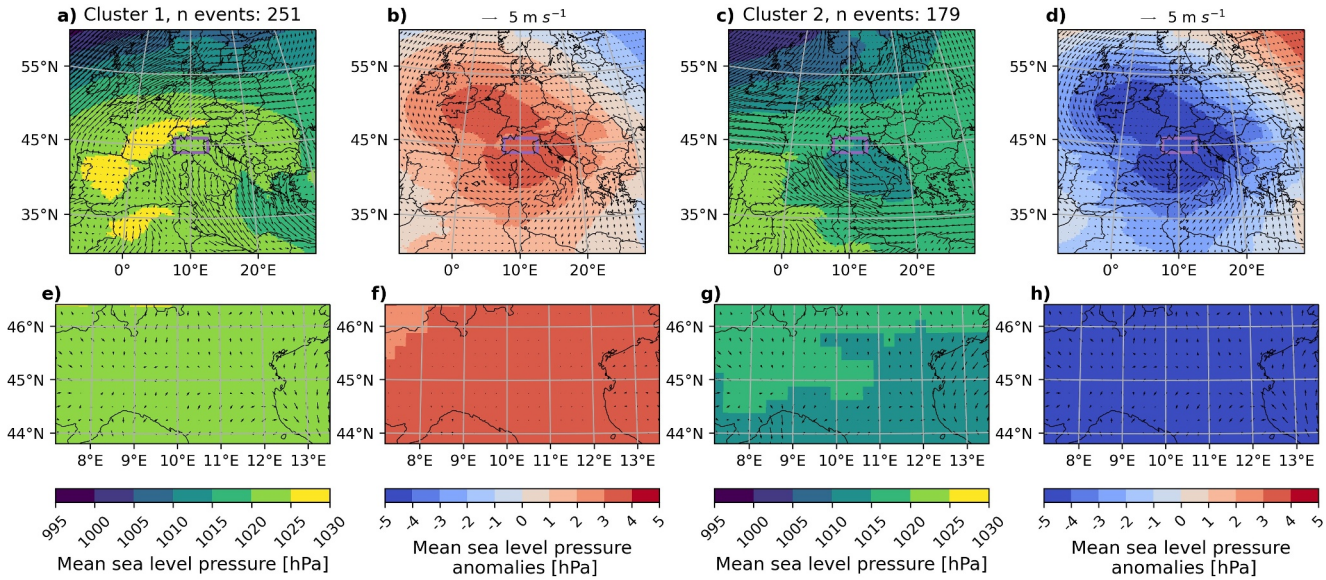

Figure 2. Mean sea level pressure (msp) (a, c, e, g) for the two clusters and cluster specific anomalies (b, d, f, h). Cluster 1 is shown in a–b and e–f, cluster 2 in c–d and g–h. Wind arrows show 10 m u and v winds. The location of the Po valley is indicated with the purple box and a zoom into the region is shown in plots e–h. Cluster-specific anomalies are created as deviations from the mean over all selected 430 FLS events.

In general, advective processes dominate FLS formation in cluster 2, as the synoptic setting is more dynamic, with a low pressure system over Italy and near surface winds transporting moist air from the Mediterranean onto the land (Figures 2g and 2h). The vertical patterns of temperature and relative humidity in cluster 2, shown by the deviation from the domain mean, are opposite from those in cluster 1. Both the boundary layer and the free troposphere are colder and moister than the domain mean (Figures 3g and 3h) and a warm anomaly is visible over the Adriatic sea (Figure 3e) with low boundary layer winds and slightly stronger northerlies in the free troposphere.

While the separation of these two clusters from a synoptic perspective (Figures 2 and 3) is adequate for most FLS events, the same synoptic conditions could also lead to different FLS types (Bari et al., 2015, 2016) and FLS formation can also be a result of combined radiative and advective processes: FLS development can start radiatively, supported by stable synoptic conditions but grows as a result of moist and cool air advection from the Mediterranean (Wobrock et al., 1992). This leads to FLS situations with low visibilities (100 m) and high liquid

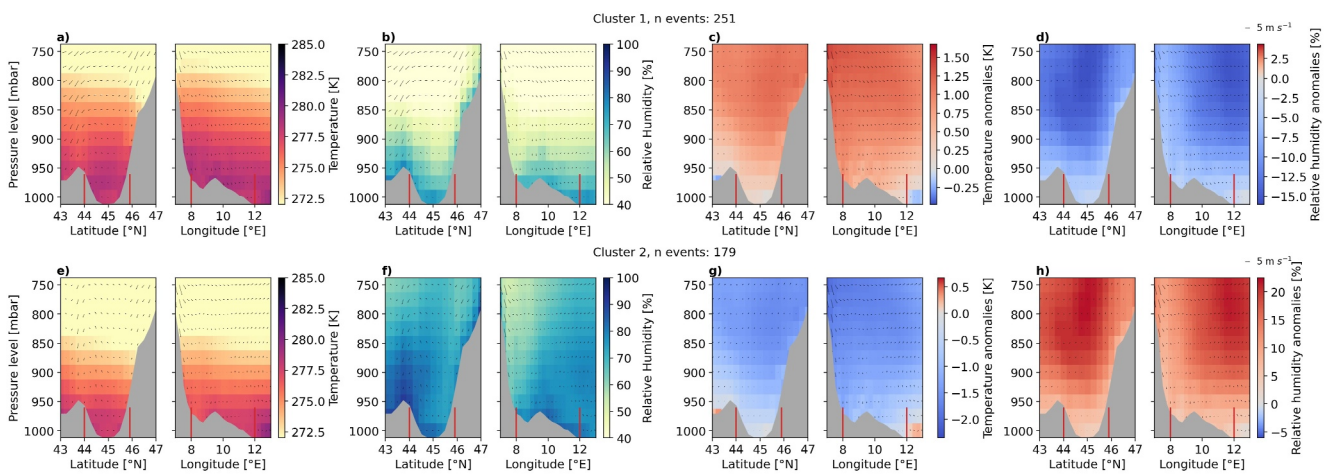

Figure 3. Vertical profiles of temperature (a), (e) and relative humidity (b), (f) and the cluster specific anomalies of temperature (c), (g) and relative humidity (d), (h) for both clusters. The latitudinal profile is averaged over 11.25°E–12.25°E and the longitudinal profile is averaged over 44.5°N–45.5°N. The red lines show the location of the Po valley. Anomalies are created as in Figure 2.

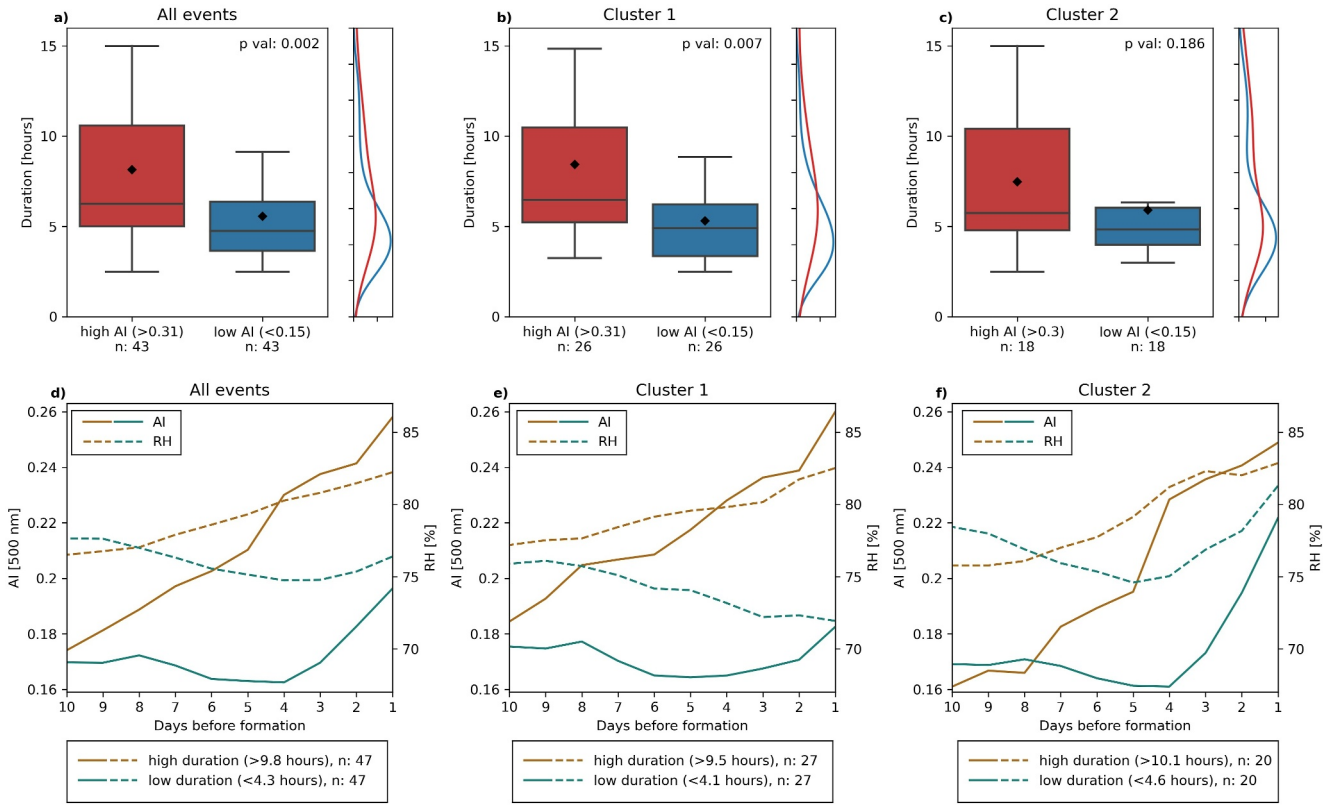

Figure 4. Distribution of FLS event duration for high and low AI values (1 day rolling mean before FLS formation) for all events (a), Cluster 1 (b) and Cluster 2 (c) and the 1–10 days rolling means of AI (solid lines) and near-ground RH (dashed line) before FLS formation on high (gold lines) and low duration (green lines) days, averaged for all events (d), Cluster 1 (e) and Cluster 2 (f). In the boxplots, the median is shown as a horizontal black line, the mean as a black diamond and outliers are removed for visibility reasons.

water content (LWC) (200 mg m^{-3}) (Bendix, 1994), resulting in highly persistent FLS events lasting several days (e.g., one FLS event in cluster 1 from 2015 to 12–23 to 2015-12-29). While using a higher number of clusters could help in further identifying the synoptic conditions leading to those mixed types (cf. Figures S4–S6 in Supporting Information S1), ground-based observations are needed to explain the corresponding processes.

3.3. Aerosol Effects on FLS Duration

Figure 4 shows the distribution of FLS event duration for high and low AI situations and the temporal development of AI and RH before FLS forms for high and low FLS duration events separately. High and low AI days are defined by the 25th and 75th percentiles of the 1 day running mean prior to FLS formation. The 25th and 75th percentile thresholds are set for all events and for each cluster separately. FLS event duration is significantly ($p < 0.01$) larger in high AI situations when considering all events and for events in cluster 1 (Figures 4a and 4b). For events in cluster 2, the difference is not significant, which can be attributed to the higher amount of (advected) low stratus situations and consequently a lower influence of near-surface aerosol loadings on FLS duration. FLS event duration is on average 2.5 hr (all events) to 3 hr (cluster 1) longer in high AI situations which is in line with modeling studies, which have shown that high aerosol loading can increase fog duration from 60 to 160 min (Maalick et al., 2016; Yan et al., 2020). The increase in FLS duration can be explained by aerosol-cloud interactions where an increase in CCN leads to an increase in fog droplets and LWC in polluted (high AI) conditions, as an increase in CCN leads more but smaller fog droplets, resulting in a reduced sedimentation velocity and a longer residue time of fog droplets (Maalick et al., 2016; Yan et al., 2021). The resulting larger cloud optical depth reduces the solar radiation reaching the surface and the sensible heat flux, leading to delayed fog dissipation (Yan et al., 2021). This can then have a positive feedback on the subsequent fog event, leading to more widespread fog formation due to lower temperatures and higher relative humidity (Yan et al., 2021).

The temporal development of AI before FLS forms, displayed by the 1–10 days running mean of AI on high and low duration days, shows a stronger increase of AI before longer FLS events (Figures 4d–4f). This pattern is especially visible in cluster 1, which can be explained by a positive feedback loop, where an accumulation of pollutants in the stable boundary layer (visible in Figure 3a) leads to a temperature decrease near the surface and an increase in the middle atmosphere, increasing the stability even further (ARI) (Gao et al., 2015). This feedback loop, where increasing aerosol loadings increase the stability of the boundary layer can then lead to an accumulation of pollutants and likely to a subsequent increase in CCN and more persistent FLS events in prolonged stable conditions. While ARI effects can also lead to earlier dissipation of fog over urban areas (Anurose et al., 2024), the magnitude of ACI effects on fog lifetime is assumed to be higher (Yan et al., 2021).

The difference between high and low AI conditions in Figure 4 is also likely to some extent influenced by different meteorological conditions (Mass et al., 2024) and confounding factors such as RH (Figures 4d–4f). Even though AI provides a size-independent measurement of aerosols, the increase of RH ahead of high FLS duration events suggests hygroscopic swelling of aerosols in high RH conditions, leading to increases in AOD (Quaas et al., 2010). Therefore, the increase in FLS persistence under high aerosol loading likely provides an upper boundary of the effect of aerosols on FLS persistence, similarly to the effect of aerosols on cloud development and cloud fraction as suggested in Gryspeerdt et al. (2014).

4. Conclusions

In this study, the FLS life cycle over the Po valley with respect to synoptic conditions and aerosol loading is investigated. Using k-means clustering on latitudinal profiles of relative humidity, 430 FLS events in winter from 2006 to 2015 are sorted into two main clusters. The analysis of the cluster-specific synoptic conditions suggest that one cluster mostly contains radiative FLS events under stable conditions and one contains advective FLS events under more dynamic conditions. We further find that in polluted (high AI) conditions, FLS duration is prolonged by up to 3 hr, which is likely due to both aerosol-cloud and aerosol-radiation interactions. As aerosol loading ahead of persistent FLS events shows a clear increasing trend 10 days ahead of FLS formation, we suggest using the temporal development of aerosol loading to improve FLS prediction models. To further disentangle aerosol effects on FLS formation, duration and dissipation, we propose combining observations and sensitivity studies of fog and aerosols, particularly in urban areas where both aerosol loading and the economic impact are high.

Conflict of Interest

The authors declare no conflicts of interest relevant to this study.

Data Availability Statement

The FLS occurrence data set has been published by Egli (2017) and is available for download. The FLS formation and dissipation time data set (Pauli et al., 2021) and the ERA5 data on pressure and on single levels (Hersbach et al., 2023a, 2023b) are also publicly available. AERONET data from the stations at Ispra, Modena and Venice was downloaded from NASA Goddard Space Flight Center (2024).

Acknowledgments
This work has received funding by the European Commission, H2020 Research Infrastructures (FORCeS (Grant 821205)) and by the German Federal Ministry for Economic Affairs and Climate Action (BMBF) in grant FKZ03EE1083C, SnowFogS. EP has been financially supported by GRACE (Graduate School for Climate and Environment). We thank Giuseppe Zibordi and Barbara Bulgarelli (Ispra and Venice) and Sergio Pugnaghi, Stefano Corradini and Sergio Teggi (Modena) and their staff for establishing and maintaining the AERONET sites at Ispra, Modena and Venice. The authors would also like to thank Michaela Schütz and Paul Zieger for fruitful discussions. We thank two anonymous reviewers for their careful and constructive reviews which have helped improve the manuscript. Open access funding enabled and organized by Projekt DEAL.

References

American Meteorological Society. (2012). *Fog*. Glossary of Meteorology.

Andersen, H., Cermak, J., Fuchs, J., Knippertz, P., Gaetani, M., Quinting, J., et al. (2020). Synoptic-scale controls of fog and low-cloud variability in the Namib Desert. *Atmospheric Chemistry and Physics*, *20*(6), 3415–3438. https://doi.org/10.5194/acp-20-3415-2020

Anurose, T. J., Jayakumar, A., Sandhya, M., Gordon, H., Aryasree, S., Mohandas, S., et al. (2024). Unraveling the mechanism of the holes in the blanket of fog over the Indo-Gangetic plains: Are they driven by urban heat islands or aerosol? *Geophysical Research Letters*, *51*(10). https://doi.org/10.1029/2023GL107252

Bari, D., Bergot, T., & El Khlifi, M. (2015). Numerical study of a coastal fog event over Casablanca, Morocco. *Quarterly Journal of the Royal Meteorological Society*, *141*(690), 1894–1905. https://doi.org/10.1002/qj.2494

Bari, D., Bergot, T., & El Khlifi, M. (2016). Local meteorological and large-scale weather characteristics of fog over the Grand Casablanca region, Morocco. *Journal of Applied Meteorology and Climatology*, *55*(8), 1731–1745. https://doi.org/10.1175/JAMC-D-15-0314.1

Bendix, J. (1993). Nebelbildung, -verteilung, und -dynamik in der Poebene - Eine Bearbeitung digitaler Wettersatellitendaten unter besonderer Berücksichtigung anwendungsorientierter Aspekte. In *Nebel im Alpenraum* (Heft 86 ed., pp. 187–301). Bonner Geographische Abhandlungen.

Bendix, J. (1994). *Fog climatology of the Po valley*. Rivista di meteorologia aeronautica.

Bergot, T. (2016). Large-eddy simulation study of the dissipation of radiation fog. *Quarterly Journal of the Royal Meteorological Society*, *142*(695), 1029–1040. https://doi.org/10.1002/qj.2706

Cermak, J., & Bendix, J. (2007). Dynamical nighttime fog/low stratus detection based on Meteosat SEVIRI data: A feasibility study. *Pure and Applied Geophysics*, *164*(6–7), 1179–1192. https://doi.org/10.1007/s00024-007-0213-8

Cermak, J., & Bendix, J. (2008). A novel approach to fog/low stratus detection using Meteosat 8 data. *Atmospheric Research*, *87*(3–4), 279–292. https://doi.org/10.1016/j.atmosres.2007.11.009

Cermak, J., Eastman, R. M., Bendix, J., & Warren, S. G. (2009). European climatology of fog and low stratus based on geostationary satellite observations. *Quarterly Journal of the Royal Meteorological Society*, *135*(645), 2125–2130. https://doi.org/10.1002/qj.503

Cuxart, J., & Jiménez, M. A. (2012). Deep radiation fog in a wide closed valley: Study by numerical modeling and remote sensing. *Pure and Applied Geophysics*, *169*(5–6), 911–926. https://doi.org/10.1007/s00024-011-0365-4

Di Antonio, L., Di Biagio, C., Foret, G., Formenti, P., Siour, G., Doussin, J. F., & Beekmann, M. (2023). Aerosol optical depth climatology from the high-resolution MAIAC product over Europe: Differences between major European cities and their surrounding environments. *Atmospheric Chemistry and Physics*, *23*(19), 12455–12475. https://doi.org/10.5194/acp-23-12455-2023

Dietz, S. J., Kneringer, P., Mayr, G. J., & Zeileis, A. (2019). Low-visibility forecasts for different flight planning horizons using tree-based boosting models. *Advances in Statistical Climatology, Meteorology and Oceanography*, *5*(1), 101–114. https://doi.org/10.5194/ascmo-5-101-2019

Egli, S. (2017). Fog and low stratus mask (Europe) [dataset]. *Laboratory for Climatology and Remote Sensing*. Retrieved from https://vhrz669.hrz.uni-marburg.de/lcrs/data_pre.do?citid=291

Egli, S., Thies, B., & Bendix, J. (2019). A spatially explicit and temporally highly resolved analysis of variations in fog occurrence over Europe. *Quarterly Journal of the Royal Meteorological Society*, *145*(721), 1721–1740. https://doi.org/10.1002/qj.3522

Egli, S., Thies, B., Drönner, J., Cermak, J., Bendix, J., Thies, B., & Bendix, J. (2017). A 10 year fog and low stratus climatology for Europe based on Meteosat Second Generation data. *Quarterly Journal of the Royal Meteorological Society*, *143*(702), 530–541. https://doi.org/10.1002/qj.2941

Fantuzi, A. (1987). Fog persistence above some airports of the north-italian plains(la persistenza della nebbia su alcuni aeroporti delle pianure dell'italia settentrionale). *Rivista di Meteorologia Aeronautica*, *47*, 117–124.

Fuchs, J., Andersen, H., Cermak, J., Pauli, E., & Roebeling, R. (2022). High-resolution satellite-based cloud detection for the analysis of land surface effects on boundary layer clouds. *Atmospheric Measurement Techniques*, *15*(14), 4257–4270. https://doi.org/10.5194/amt-15-4257-2022

Fuzzi, S., Facchini, M. C., Orsi, G., Bonforte, G., Martinotti, W., Ziliani, G., et al. (1996). The NEVALPA project: A regional network for fog chemical climatology over the Po valley basin. *Atmospheric Environment*, *30*(2), 201–213. https://doi.org/10.1016/1352-2310(95)00298-D

Gao, Y., Zhang, M., Liu, Z., Wang, L., Wang, P., Xia, X., et al. (2015). Modeling the feedback between aerosol and meteorological variables in the atmospheric boundary layer during a severe fog-haze event over the North China Plain. *Atmospheric Chemistry and Physics*, *15*(8), 4279–4295. https://doi.org/10.5194/acp-15-4279-2015

Gautam, R., & Singh, M. K. (2018). Urban heat island over Delhi punches holes in widespread fog in the Indo-Gangetic plains. *Geophysical Research Letters*, *45*(2), 1114–1121. https://doi.org/10.1002/2017GL076794

Gilardoni, S., Massoli, P., Giulianelli, L., Rinaldi, M., Paglione, M., Pollini, F., et al. (2014). Fog scavenging of organic and inorganic aerosol in the Po Valley. *Atmospheric Chemistry and Physics*, *14*(13), 6967–6981. https://doi.org/10.5194/acp-14-6967-2014

Giulianelli, L., Gilardoni, S., Tarozzi, L., Rinaldi, M., Decesari, S., Carbone, C., et al. (2014). Fog occurrence and chemical composition in the Po valley over the last twenty years. *Atmospheric Environment*, *98*, 394–401. https://doi.org/10.1016/j.atmosenv.2014.08.080

Glickman, T. (2000). *Glossary of meteorology (2nd ed.)*. American Meteorological Society.

Gottlieb, T. R., Eckardt, F. D., Venter, Z. S., & Cramer, M. D. (2019). The contribution of fog to water and nutrient supply to Arthraerua leubnitziae in the central Namib Desert, Namibia. *Journal of Arid Environments*, *161*, 35–46. https://doi.org/10.1016/j.jaridenv.2018.11.002

Gryspeerdt, E., Stier, P., & Partridge, D. G. (2014). Satellite observations of cloud regime development: The role of aerosol processes. *Atmospheric Chemistry and Physics*, *14*(3), 1141–1158. https://doi.org/10.5194/acp-14-1141-2014

Gultepe, I., Tardif, R., Michaelides, S. C., Cermak, J., Bott, A., Bendix, J., et al. (2007). Fog research: A review of past achievements and future perspectives. *Pure and Applied Geophysics*, *164*(6–7), 1121–1159. https://doi.org/10.1007/s00024-007-0211-x

Hartigan, J. A., & Wong, M. A. (1979). Algorithm as 136: A K-means clustering algorithm. *Applied Statistics*, *28*(1), 100. https://doi.org/10.2307/2346830

Hersbach, H., Bell, B., Berrisford, P., Biavati, G., Horányi, A., Muñoz Sabater, J., et al. (2023a). ERA5 hourly data on pressure levels from 1940 to present. *Copernicus Climate Change Service (C3S) Climate Data Store (CDS)*. [dataset]. https://doi.org/10.24381/cds.bd0915c6

Hersbach, H., Bell, B., Berrisford, P., Biavati, G., Horányi, A., Muñoz Sabater, J., et al. (2023b). ERA5 hourly data on single levels from 1940 to present. *Copernicus Climate Change Service (C3S) Climate Data Store (CDS)*. [dataset]. https://doi.org/10.24381/cds.adbb2d47

Holben, B. N., Eck, T. F., Slutsker, I., Tanré, D., Buis, J. P., Setzer, A., et al. (1998). AERONET—A federated instrument network and data archive for aerosol characterization. *Remote Sensing of Environment*, *66*(1), 1–16. https://doi.org/10.1016/S0034-4257(98)00031-5

Kneringer, P., Dietz, S. J., Mayr, G. J., & Zeileis, A. (2019). Probabilistic nowcasting of low-visibility procedure states at Vienna international airport during cold season. *Pure and Applied Geophysics*, *176*(5), 2165–2177. https://doi.org/10.1007/s00024-018-1863-4

Köhler, C., Steiner, A., Saint-Drenan, Y. M., Ernst, D., Bergmann-Dick, A., Zirkelbach, M., et al. (2017). Critical weather situations for renewable energies – Part B: Low stratus risk for solar power. *Renewable Energy*, *101*, 794–803. https://doi.org/10.1016/j.renene.2016.09.002

Leigh, R. J., Drake, L., & Thampapillai, D. J. (1998). An economic analysis of terminal aerodrome forecasts with special reference to Sydney airport. *Journal of Transport Economics and Policy*, *32*(3), 377–392.

Lyapustin, A., Wang, Y., Korkin, S., & Huang, D. (2018). MODIS Collection 6 MAIAC algorithm. *Atmospheric Measurement Techniques*, *11*(10), 5741–5765. https://doi.org/10.5194/amt-11-5741-2018

Maalick, Z., Kühn, T., Korhonen, H., Kokkola, H., Laaksonen, A., & Romakkaniemi, S. (2016). Effect of aerosol concentration and absorbing aerosol on the radiation fog life cycle. *Atmospheric Environment*, *133*, 26–33. https://doi.org/10.1016/j.atmosenv.2016.03.018

Mass, A., Andersen, H., Cermak, J., Formenti, P., Pauli, E., & Quinting, J. (2024). A satellite-based analysis of semi-direct effects of biomass burning aerosols on fog and low cloud dissipation in the Namib Desert. *EGUsphere*, *2024*, 1–25. https://doi.org/10.5194/egusphere-2024-1627

Mitchell, D., Henschel, J. R., Hetem, R. S., Wassenaar, T. D., Strauss, W. M., Hanrahan, S. A., & Seely, M. K. (2020). Fog and fauna of the Namib Desert: Past and future. *Ecosphere*, *11*(1). https://doi.org/10.1002/ecs2.2996

Nakajima, T., Higurashi, A., Kawamoto, K., & Penner, J. E. (2001). A possible correlation between satellite-derived cloud and aerosol microphysical parameters. *Geophysical Research Letters*, *28*(7), 1171–1174. https://doi.org/10.1029/2000GL012186

NASA Goddard Space Flight Center. (2024). Aerosol optical depth (V3) - Solar [dataset]. *NASA Goddard Space Flight Center*. Retrieved from https://aeronet.gsfc.nasa.gov/new_web/webtool_aod_v3.html

O'Neill, N. T., Eck, T. F., Smirnov, A., Holben, B. N., & Thulasiraman, S. (2003). Spectral discrimination of coarse and fine mode optical depth. *Journal of Geophysical Research*, *108*(17), 1–15. https://doi.org/10.1029/2002jd002975

Pagowski, M., Gultepe, I., & King, P. (2004). Analysis and modeling of an extremely dense fog event in southern Ontario. *Journal of Applied Meteorology*, *43*(1), 3–16. https://doi.org/10.1175/1520-0450(2004)043<0003:aamoae>2.0.co;2

Pauli, E., Andersen, H., Bendix, J., Cermak, J., & Egli, S. (2020). Determinants of fog and low stratus occurrence in continental central Europe – A quantitative satellite-based evaluation. *Journal of Hydrology*, *591*, 1–15. https://doi.org/10.1016/j.jhydrol.2020.125451

Pauli, E., Cermak, J., & Andersen, H. (2021). Satellite-based fog and low stratus cloud formation and dissipation times data set. *KIT-Bibliothek, KITopenData*. [dataset]. https://doi.org/10.5445/IR/1000141293

Pauli, E., Cermak, J., & Andersen, H. (2022). A satellite-based climatology of fog and low stratus formation and dissipation times in central Europe. *Quarterly Journal of the Royal Meteorological Society*, *148*(744), 1439–1454. https://doi.org/10.1002/qj.4272

Pauli, E., Cermak, J., Andersen, H., & Fuchs, J. (2024). An analysis of fog and low stratus life-cycle regimes over central Europe. *Quarterly Journal of the Royal Meteorological Society*, *150*(761), 1–15. https://doi.org/10.1002/qj.4714

Pauli, E., Cermak, J., & Teuling, A. J. (2022). Enhanced nighttime fog and low stratus occurrence over the Landes forest, France. *Geophysical Research Letters*, *49*(5). https://doi.org/10.1029/2021GL097058

Pérez-Díaz, J. L., Ivanov, O., Peshev, Z., Álvarez-Valenzuela, M. A., Valiente-Blanco, I., Evgenieva, T., et al. (2017). Fogs: Physical basis, characteristic properties, and impacts on the environment and human health. *Water (Switzerland)*, *9*(807), 1–21. https://doi.org/10.3390/w9100807

Pohl, M. J., Lehnert, L. W., Thies, B., Seeger, K., Berdugo, M. B., Gradstein, S. R., et al. (2023). Valleys are a potential refuge for the Amazon lowland forest in the face of increased risk of drought. *Communications Earth and Environment*, *4*(1), 1–10. https://doi.org/10.1038/s43247-023-00867-6

Poku, C., Ross, A. N., Blyth, A. M., Hill, A. A., & Price, J. D. (2019). How important are aerosol–fog interactions for the successful modelling of nocturnal radiation fog? *Weather*, *74*(7), 237–243. https://doi.org/10.1002/wea.3503

Price, J. D. (2019). On the formation and development of radiation fog: An observational study. *Boundary-Layer Meteorology*, *172*(2), 167–197. https://doi.org/10.1007/s10546-019-00444-5

Putaud, J. P., Cavalli, F., Dos Santos, M., & Dell'Acqua, A. (2014). Long-term trends in aerosol optical characteristics in the Po Valley, Italy. *Atmospheric Chemistry and Physics*, *14*(17), 9129–9136. https://doi.org/10.5194/acp-14-9129-2014

Quaas, J., Stevens, B., Stier, P., & Lohmann, U. (2010). Interpreting the cloud cover-Aerosol optical depth relationship found in satellite data using a general circulation model. *Atmospheric Chemistry and Physics*, *10*(13), 6129–6135. https://doi.org/10.5194/acp-10-6129-2010

Ramanathan, V., Crutzen, P. J., Kiehl, J. T., & Rosenfeld, D. (2001). Aerosols, climate, and the hydrological cycle. *Science*, *294*(December), 2119–2125. https://doi.org/10.1126/science.1064034

Roach, W. (1995). Back to basics: Fog: Part 2 - the formation and dissipation of land fog. *Weather*, *50*(1), 7–11. https://doi.org/10.1002/j.1477-8696.1995.tb06053.x

Rousseeuw, P. J. (1987). Silhouettes: A graphical aid to the interpretation and validation of cluster analysis. *Journal of Computational and Applied Mathematics*, *20*, 53–65. https://doi.org/10.1016/0377-0427(87)90125-7

Scherrer, S. C., & Appenzeller, C. (2014). Fog and low stratus over the Swiss Plateau-a climatological study. *International Journal of Climatology*, *34*(3), 678–686. https://doi.org/10.1002/joc.3714

Scotto, F., Bacco, D., Lasagni, S., Trentini, A., Poluzzi, V., & Vecchi, R. (2021). A multi-year source apportionment of PM2.5 at multiple sites in the southern Po Valley (Italy). *Atmospheric Pollution Research*, *12*(11), 101192. https://doi.org/10.1016/j.apr.2021.101192

Stolaki, S., Haeffelin, M., Lac, C., Dupont, J. C., Elias, T., & Masson, V. (2015). Influence of aerosols on the life cycle of a radiation fog event. A numerical and observational study. *Atmospheric Research*, *151*, 146–161. https://doi.org/10.1016/j.atmosres.2014.04.013

Twomey, S. (1977). The influence of pollution on the shortwave albedo of clouds. *Journal of the Atmospheric Sciences*, *34*(7), 1149–1152. https://doi.org/10.1175/1520-0469(1977)034<1149:tiopot>2.0.co;2

Wobrock, W., Schell, D., Maser, R., Kessel, M., Jaeschke, W., Fuzzi, S., et al. (1992). Meteorological characteristics of the Po Valley fog. *Tellus B: Chemical and Physical Meteorology*, *44*(5), 469. https://doi.org/10.3402/tellusb.v44i5.15562

Yan, S., Zhu, B., Huang, Y., Zhu, J., Kang, H., Lu, C., & Zhu, T. (2020). To what extents do urbanization and air pollution affect fog? *Atmospheric Chemistry and Physics*, *20*(9), 5559–5572. https://doi.org/10.5194/acp-20-5559-2020

Yan, S., Zhu, B., Zhu, T., Shi, C., Liu, D., Kang, H., et al. (2021). The effect of aerosols on fog lifetime: Observational evidence and model simulations. *Geophysical Research Letters*, *48*(2). https://doi.org/10.1029/2020GL091156

Ye, H. (2009). The influence of air temperature and atmospheric circulation on winter fog frequency over Northern Eurasia. *International Journal of Climatology*, *29*(5), 729–734. https://doi.org/10.1002/joc.1741